FoxO3 regulates neuronal reprogramming of cells from postnatal and aging mice

Henrik Ahlenius[a,1,2], Soham Chanda[a,b,1], Ashley E. Webb[c,3], Issa Yousif[a], Jesse Karmazin[a], Stanley B. Prusiner[d,e,f], Anne Brunet[c], Thomas C. Südhof[b,g,4], and Marius Wernig[a,4]

[a]Institute for Stem Cell Biology and Regenerative Medicine and Department of Pathology, Stanford University School of Medicine, Stanford, CA 94305; [b]Department of Molecular and Cellular Physiology, Stanford University School of Medicine, Stanford, CA 94305; [c]Department of Genetics, Stanford University School of Medicine, Stanford, CA 94305; [d]Institute for Neurodegenerative Diseases, University of California, San Francisco, CA 94158; [e]Department of Neurology, University of California, San Francisco, CA 94158; [f]Department of Biochemistry and Biophysics, University of California, San Francisco, CA 94158; and [g]Howard Hughes Medical Institute, Stanford University School of Medicine, Stanford, CA 94305

Contributed by Thomas C. Südhof, June 1, 2016 (sent for review August 24, 2015; reviewed by Anton Maximov, Yi E. Sun, and Li-Huei Tsai)

We and others have shown that embryonic and neonatal fibroblasts can be directly converted into induced neuronal (iN) cells with mature functional properties. Reprogramming of fibroblasts from adult and aged mice, however, has not yet been explored in detail. The ability to generate fully functional iN cells from aged organisms will be particularly important for in vitro modeling of diseases of old age. Here, we demonstrate production of functional iN cells from fibroblasts that were derived from mice close to the end of their lifespan. iN cells from aged mice had apparently normal active and passive neuronal membrane properties and formed abundant synaptic connections. The reprogramming efficiency gradually decreased with fibroblasts derived from embryonic and neonatal mice, but remained similar for fibroblasts from postnatal mice of all ages. Strikingly, overexpression of a transcription factor, forkhead box O3 (FoxO3), which is implicated in aging, blocked iN cell conversion of embryonic fibroblasts, whereas knockout or knockdown of FoxO3 increased the reprogramming efficiency of adult-derived but not of embryonic fibroblasts and also enhanced functional maturation of resulting iN cells. Hence, FoxO3 has a central role in the neuronal reprogramming susceptibility of cells, and the importance of FoxO3 appears to change during development.

aging | reprogramming | induced neuronal cells

Recent advances in direct reprogramming have demonstrated the feasibility of converting fibroblasts and other terminally differentiated lineages into induced neuronal (iN) cells (1–8). iN cells display elaborate morphologies typical of neurons, express pan-neuronal markers, exhibit hallmarks of functional neurons in that they fire action potentials and form abundant synapses, and, thus, provide a great opportunity for studying the cellular phenotypes of disease-associated genetic mutations (9). To date, most studies used embryonic or early postnatal fibroblasts for reprogramming purposes, but for clinical applications, and in particular for modeling age-related neurodegenerative diseases, it would be preferable to generate iN cells from adult and aged animals.

Lineage conversion from aged cells is often challenging, probably due to epigenetic changes during aging. For example, aging has been shown to impair conversion of somatic cells into induced pluripotent stem cells (3, 10–12). A recent elegant paper demonstrated successful conversion of fibroblasts from old individuals, but cellular properties were not compared between different age groups (13). In embryonic fibroblasts, overexpression of three transcription factors, Brn2, Ascl1, and Myt1l (BAM), efficiently generates iN cells with mature, functional properties within 2 wk (1). Genomic studies and chromatin characterization experiments of fibroblasts shortly after BAM factor expression revealed unique pioneer factor properties of Ascl1, which led to our observation that Ascl1 alone is sufficient to generate functional iN cells, albeit slower and with lower efficiency than when all three BAM transcription factors are used (14, 15). Recently, we observed that the longevity-associated forkhead transcription factor, FoxO3, shares common genomic targets with Ascl1 and, when overexpressed, significantly impairs iN cell reprogramming (16). FoxO3 functions downstream of the insulin/IGF signaling pathway and has also been shown to maintain adult neural precursor cell homeostasis (17–19). Thus, FoxO3 might indirectly also affect neurogenesis.

Our aims for the present study were threefold: first, we wanted to assess whether it is possible to reprogram fibroblasts from aged mice into neurons; second, we wanted to elucidate whether aging affects the dynamics of neuronal conversion of fibroblasts; and finally, we wanted to investigate whether intrinsic, aging-associated factors, such as members of the FoxO family of transcription factors, influence iN cell formation in an age-dependent manner.

Results

Generation of Functional iN Cells from Fibroblasts of Old Mice. We have shown that forced expression of a pool of three transcription factors, Brn2, Ascl1, and Myt1l, successfully converts mouse embryonic fibroblasts (MEFs) and early postnatal tail-tip fibroblasts (TTFs) into iN cells (1). To establish whether aging fibroblasts can also be converted into iN cells, we derived cultures from tails of 17- to 20-month-old Tau:EGFP mice that express EGFP from the endogenous, neuron-specific *Tau* locus (20). The tail-tip fibroblasts were then lentivirally transduced with BAM transcription factors.

Significance

Direct reprogramming of nonneuronal cells into induced neuronal (iN) cells has been of great interest for its potential applications in neurological disease modeling. Although this approach is well-established using cells from embryonic and neonatal animals, its applicability for cells from adult and aged animals has remained unexplored. This study demonstrates that iN cells can be efficiently generated from aging animals, but that age-dependent roadblocks which depend on the transcription factor FoxO3 affect the reprogramming efficiency and functional maturation of iN cell properties. Eliminating these roadblocks may be useful for modeling age-related neurological disorders using iN cells.

Author contributions: H.A., S.C., S.B.P., A.B., T.C.S., and M.W. designed research; H.A., S.C., A.E.W., I.Y., and J.K. performed research; A.B. contributed new reagents/analytic tools; H.A., S.C., A.E.W., J.K., T.C.S., and M.W. analyzed data; and H.A., S.C., and M.W. wrote the paper.

Reviewers: A.M., The Scripps Research Institute; Y.E.S., University of California, Los Angeles; and L.-H.T., Massachusetts Institute of Technology.

The authors declare no conflict of interest.

[1]H.A. and S.C. contributed equally to this work.

[2]Present address: Department of Clinical Sciences, Lund Stem Cell Center, University Hospital BMC B10, SE-221 84 Lund, Sweden.

[3]Present address: Department of Molecular Biology, Cell Biology and Biochemistry, Brown University, Providence, RI 02903.

[4]To whom correspondence may be addressed. Email: tcs1@stanford.edu or wernig@stanford.edu.

This article contains supporting information online at www.pnas.org/lookup/suppl/doi:10.1073/pnas.1607079113/-/DCSupplemental.

Three weeks later, we detected bright EGFP$^+$ cells with clear neuronal morphologies and expression of the pan-neuronal marker Tuj1 (Fig. 1*A*). Electrophysiological characterization demonstrated that TTF-derived iN (TTF iN) cells generated from aged animals were functional in terms of firing action potentials (APs) and exhibiting voltage-gated sodium and potassium currents (Fig. 1*B*). Thus, the BAM reprogramming factors are capable of converting fibroblasts from aged donors into functional neurons.

Developmental Stage but Not Adult Aging Impairs iN Cell Reprogramming. To more systematically evaluate the impact of aging on reprogramming efficiency of fibroblasts, we derived TTFs from mice of different ages including embryonic (MEF), postnatal (4 d), young adult (3 mo), middle aged (10 and 15 mo), and aged (25 mo) mice. Following BAM transduction, fibroblasts from all ages were able to form Tuj1 and Map2 immunopositive iN cells with neuronal morphology (Fig. 1*C*). However, the reprogramming efficiency and

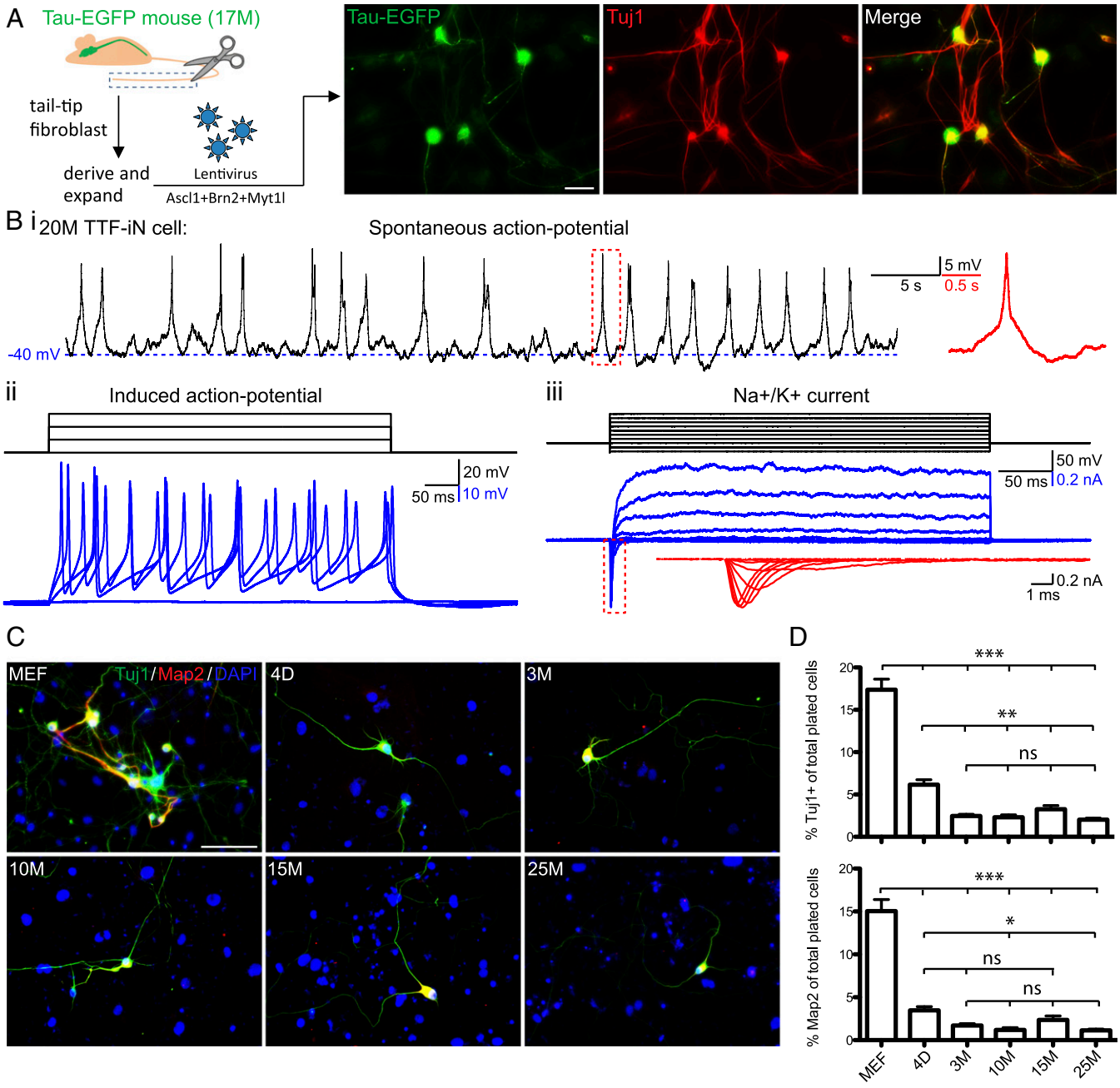

Fig. 1. Fibroblasts from postnatal and adult mice are less susceptible to iN cell reprogramming than MEFs. (*A*) Experimental approach (*Left*) and image of iN cells (*Right*) generated from TTFs of a 17-mo-old (17M) Tau-EGFP animal. Micrograph showing Tau-EGFP epifluorescence (green) and immunofluorescence detection with Tuj1 antibodies (red). (Scale bar, 30 μm.) (*B*) Sample traces of spontaneous AP firing (*i*), current-pulse–induced AP (*ii*), and voltage-gated Na^+ and K^+ currents (*iii*) recorded from TTF iN cells reprogrammed from a 20-mo-old animal (20M TTF-iN cell). *Insets* in red, magnified view of corresponding boxed area. (*C*) Representative images (*Left*) for Tuj1 (green) and Map2 (red) immunoreactivity of TTF iN cells generated from embryonic (MEF), postnatal (4 d old; 4D), adult (3 mo old; 3M), middle aged (10 and 15 mo old; 10M and 15M, respectively) and aged (25 mo old; 25M) animals, 3 wk after induction. (Scale bar, 50 μm.) (*D*) Average fractions of Tuj1$^+$ (*Top Right*) and Map2$^+$ (*Bottom Right*) cells 3 wk after infection of initially plated cells. Data are presented as means ± SEM ($n = 3$–5 experiments with three technical replicates each). Significance was determined by using one-way ANOVA with Bonferroni post hoc test (*$P < 0.05$; **$P < 0.01$; ***$P < 0.005$; ns, not significant).

dynamics of iN cell generation were reduced dramatically in postnatal cells compared with MEFs and showed a further slight decrease in subsequent age-groups tested (Fig. 1 *C* and *D* and Fig. S1).

To test the effect of aging on functional maturation of iN cells, we performed patch-clamp recordings from postnatal, juvenile, and aging adult TTF iN cells and directly compared their intrinsic membrane properties with those of MEF iN cells. We noticed that TTF iN cells generated from aging mice displayed a consistent increase in the failure rate for AP firing (Fig. 2*A*). Moreover, quantification of intrinsic membrane properties indicated a less mature state of iN cells from aged mice, such as a less polarized resting membrane potential (V_{rest}), a higher membrane resistance (R_m), and a lower capacitance (C_m) (Fig. 2*B*). Finally, when cocultured with mouse primary hippocampal neurons (Fig. S2), TTF iN cells derived from juvenile and aged mice showed a significant decrease in both the frequency and amplitude of spontaneous AMPA receptor-(AMPAR-) mediated miniature excitatory postsynaptic currents (mEPSCs) compared to MEF iN cells (Fig. 2*C*). When excitatory postsynaptic currents (EPSCs) were evoked by APs of surrounding cells with an extracellular stimulation electrode, thus activating the majority of synapses projecting onto the recorded cell, we observed a steep decrease in AMPAR-mediated synaptic transmission between MEF-iN and neonatal TTF-iN cells and a further substantial decrease between neonatal TTF-iN and adult TTF-iN cells (Fig. 2*D*). As with other parameters, there was no significant difference between TTF-iN cells from 3- or 25-mo-old mice (Fig. 2*D*).

Thus, the conversion effciency massively decreases when fibroblasts are derived from postnatal tail tips instead of embryos, but decreases surprisingly little when fibroblasts are derived from aging mice instead of neonatal mice (Figs. 1*D* and 2 *B*–*D* and Fig. S3). The small differences in iN cell reprogramming efficiency between young and aged adult fibroblasts are in accordance with published findings on neuronal differentiation from neural stem/progenitor cells (NSPCs). Similar to what we find for reprogramming, embryonic NSPCs differentiated more efficiently into neurons than adult NSPCs, but no difference was detected between young and aged adult NSPCs (21).

Several Aging-Associated Cellular Features Correlate with Reduced Reprogrammability. We next monitored a number of qualitative aging-associated parameters. In a similar context, induced pluripotent stem (iPS) cell reprogramming has been shown to be strongly influenced by cell proliferation and senescence (10, 22, 23). We therefore wondered whether these two factors also affect the quality of the donor fibroblasts derived from mice of different ages, which may influence their susceptibility to iN cell reprogramming. As expected, a 4-h pulse staining with 5-ethynyl-2′-deoxyuridine (EdU) revealed a decreased cell proliferation rate in fibroblasts as a function of the age of the donor mice (Fig. 3 *A* and *B*). Staining with senescence-associated β-galactosidase (SA-β-Gal) indicated that aging fibroblasts undergo a parallel significant increase in cellular senescence (Fig. 3 *A* and *B*). Accordingly, we observed a strong increase in mRNA expression levels of the senescence-associated genes *p16* and *p19* in aged donor fibroblasts (Fig. 3*B*). Finally, quantification of plating and infection efficiency demonstrated a significant decrease of both parameters in TTFs compared with MEFs (Fig. 3 *C* and *D*).

In summary, these findings suggest that the combination of lower proliferation, plating, and infection rates, and increased senescence, is responsible for the decreased reprogramming efficiency of TTFs derived from aging mice compared with MEFs.

Loss of FoxO3 Improves Neuronal Conversion of Fibroblasts from Aging Mice. Given the lower efficiency of BAM-induced iN cell conversion of adult fibroblasts, we sought to find means to improve reprogramming. Our previous studies indicated that of the three BAM transcription factors originally identified, Ascl1 is the main driver of iN cell reprogramming (1, 14, 15). Of note, Ascl1 alone is sufficient to induce iN cell reprogramming in fibroblasts (14, 15). We had observed earlier that FoxO3, a longevity-associated transcription factor, shares genomic targets with Ascl1 and inhibits

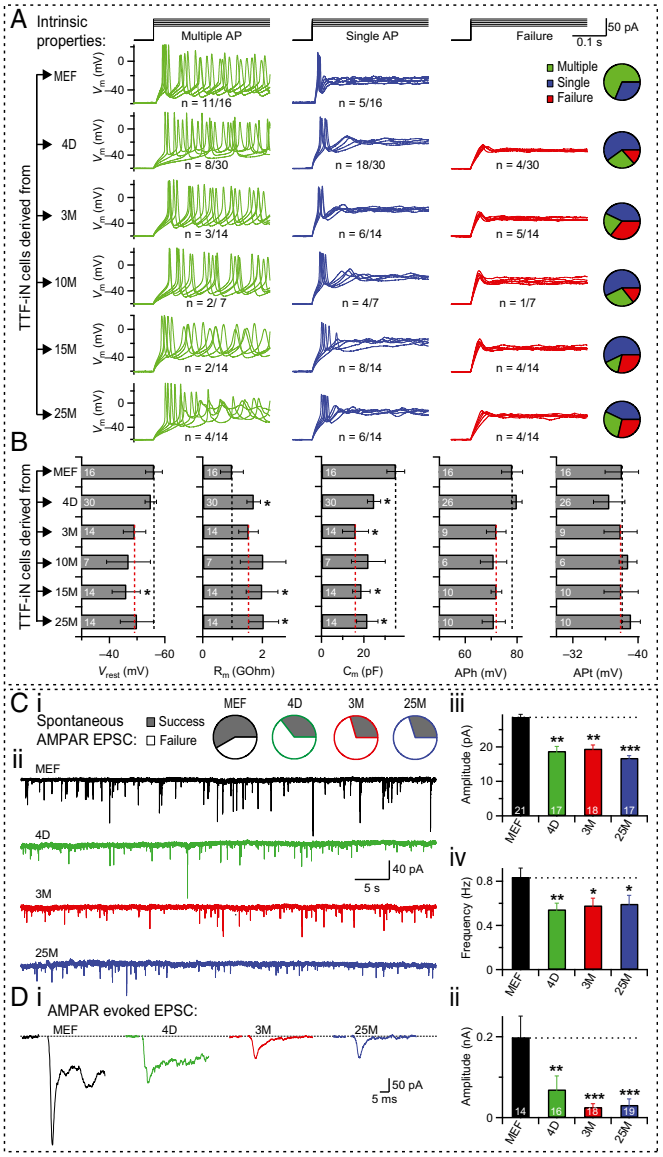

Fig. 2. iN cells derived from TTFs are functionally less mature than iN cells derived from MEFs. (*A*) Example traces of AP generation by TTF iN cells derived from animals of different ages (MEF, 4D, 3M, 10M, 15M, and 25M), as recorded in current-clamp mode, 3 wk after BAM transduction. Step-current (black) induced AP patterns: multiple AP (green), single AP (blue), or failure to generate AP (red). Pie charts indicate fraction of cells with corresponding firing patterns. *n* = number of cells with qualitatively similar AP firing property/total number of patched cells with elaborate neuronal morphology. (*B*) Average values of the intrinsic membrane properties of TTF iN cells from different ages (*y* axis) plotted as mean ± SEM. Parameters (from *left* to *right*) include resting membrane-potential (V_{rest}), membrane resistance (R_m), capacitance (C_m), AP height (APh), and AP threshold (APt). Asterisks indicate significant differences (*n* = numbers indicated on bar graphs, $*P < 0.05$, Student's *t* test) from corresponding embryonic condition (black dotted line). No significant differences were found between 3M (red dotted line) and older age groups for any parameter tested. (*C*) Spontaneous AMPAR-mediated EPSCs, as probed by voltage-clamp recordings from MEF (black), 4D (green), 3M (red), and 25M (blue) TTF iN cells. Pie charts represent ratio of cells with (gray fraction) or without (white fraction) synaptic response (*i*). Sample traces of spontaneous EPSCs recorded (*ii*), and average values of EPSC amplitude (*iii*), and frequency (*iv*) presented as mean ± SEM (*n* = numbers associated with bar graphs). Asterisks, significant difference ($*P < 0.05$, $**P < 0.01$, $***P < 0.005$, Student's *t* test), compared with the MEF condition (dotted line). (*D*) Evoked AMPAR-mediated EPSCs recorded from MEF iN cells (black), and iN cells derived from 4D (green), 3M (red), and 25M (blue) animals. Example traces (*i*) and average EPSC amplitudes (mean ± SEM) (*ii*) of each condition are plotted. Asterisks indicate significant difference (*n* = indicated on bar graphs, $**P < 0.01$, $***P < 0.005$, Student's *t* test) between MEF and aging conditions.

some of the Ascl1 target genes (16). Indeed, we confirmed that overexpression of FoxO3 impaired BAM-mediated neurogenesis from MEFs (Fig. 4*A*). In light of these findings, we wondered whether deletion of FoxO3 could improve neuronal conversion of TTFs derived from aging mice.

To this end, we first evaluated the expression levels of FoxO transcription factor genes (*FoxO1*, *FoxO3*, *FoxO4*, and *FoxO6*) in fibroblasts. Our quantitative RT-PCR (qRT-PCR) assay revealed that all family members were robustly expressed in MEFs and in TTFs derived from postnatal and adult mice (Fig. S4), as reported for skeletal muscle (24). We next derived MEFs, and adult TTFs from WT and FoxO3$^{-/-}$ littermate mice of various age groups. Unexpectedly, germ-line loss of FoxO3 also reduced *FoxO6* expression without affecting *FoxO1* or *FoxO4* mRNA levels (Fig. S4), indicating a genetic interaction between the *FoxO3* and *FoxO6* genes. Upon BAM factor induction, both WT and FoxO3$^{-/-}$ TTFs were reprogrammed into iN cells for all age groups tested. For TTFs derived from young and aged mice, but not for MEFs, we detected a significant increase in the number of Map2^{+} iN cells transdifferentiated from FoxO3$^{-/-}$ TTFs compared with WT TTFs (Fig. 4 *B* and *C*). Surprisingly, this increase in efficiency was not due to differences in infectability, proliferation, or senescence rates between WT and FoxO3$^{-/-}$ TTFs (Fig. S5). In addition, shRNA-mediated knockdown of FoxO3 in 3M TTFs also significantly increased the reprogramming efficiency of iN cells (Fig. 4*D*). Thus, the increase in reprogramming efficiency appears to be a direct consequence of reduced *FoxO3* transcriptional activity in adult fibroblasts and cannot be explained by secondary changes in adult cells devoid of FoxO3 since the beginning of embryonic development.

Finally, to test whether loss of FoxO3 also has an effect on the functional properties of iN cells, we performed current-clamp recordings from iN cells derived from WT and FoxO3$^{-/-}$ TTFs. A larger fraction of FoxO3$^{-/-}$ iN cells generated from TTFs of different age groups fired APs than of WT iN cells; this difference was absent in a comparison between FoxO3$^{-/-}$ and WT iN cells generated from MEFs (Fig. 4 *E* and *F*). Concordantly, iN cells from adult FoxO3$^{-/-}$ TTFs but not from MEFs showed a lower V_{rest} and an increased AP height compared with corresponding WT conditions (Fig. 4*G*). Thus, loss of FoxO3 improves iN cell reprogramming efficiency and functional maturation of iN cells selectively from adult but not embryonic fibroblasts.

Discussion

Lineage conversion of cells from adult animals in general has proven difficult. For example, the iPS cell reprogramming efficiency and kinetics were significantly reduced for cells from older compared with younger animals (3, 10–12). Furthermore, senescence and proliferative capacity have also been shown to influence iPS cell reprogramming (10, 22, 23). In agreement with these observations, our findings on iN cell reprogramming also suggest an inverse correlation between development and cellular reprogrammability. Remarkably, however, we did not detect any significant difference in the efficiency of reprogramming or function of iN cells from fibroblasts derived from young or aging mice. This finding is in accordance with the finding that the neuronal differentiation capacity of endogenous neural stem cells did not change from adult to aged animals, and that once mature neurons had formed, there were no detectable differences in their function (21).

The cell-biological mechanisms that cause aging remain largely a mystery. Presumably, a complex combination of many different changes is responsible for the variety of phenotypical and functional alterations induced by aging. Therefore, we were surprised to note that a simple genetic manipulation significantly increased iN cell reprogramming susceptibility in fibroblasts derived from adult but not embryonic mice. Specifically, germ-line loss of the longevity-associated transcription factor FoxO3 increased both conversion efficiency and function of iN cells from adult and aged fibroblasts. This effect was not due to differences in infection rate, proliferation, or level of senescence of the donor fibroblasts. Rather, our knockdown experiments suggest that this effect may involve a direct molecular mechanism of FoxO3 to inhibit the induction of the neuronal program induced by the reprogramming factors. This hypothesis is supported by our previous findings that FoxO3 shares genomic targets with the iN cell reprogramming transcription factor Ascl1 and inhibits its transcription and neurogenic effect when overexpressed (16). We thus speculate that by removing FoxO3 from cells, Ascl1 can exert its full neurogenic potential and, thus, more efficiently reprogram fibroblasts.

Remarkably, the effect of FoxO3 on iN cell reprogramming was not observed in embryonic fibroblasts despite robust *FoxO3* expression. Moreover, the reduction of *FoxO6* levels in FoxO3$^{-/-}$

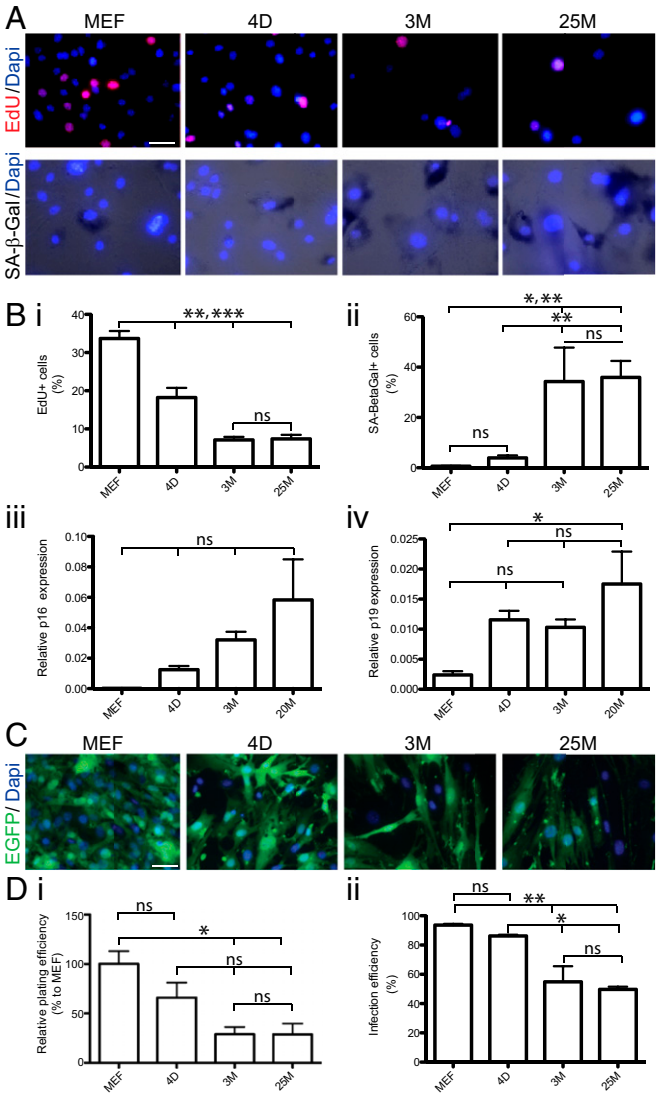

Fig. 3. Aging-associated features in donor fibroblasts. (*A*) Representative images indicating age-dependent decrease of EdU incorporation (EdU staining in red, *Top*) and increase in senescence associated β-Gal activity (black staining, *Bottom*) in fibroblasts from different age groups (MEFs, 4D, 3M, and 25M, *Left* to *Right*) counterstained with DAPI (blue). (*B*) Average bar graphs indicate means ± SEM of percentages of EdU^{+} (*i*), SA-β-Gal^{+} (*ii*) fibroblasts and average relative mRNA levels for senescence markers p16 (*iii*) and p19 (*iv*) measured by qRT-PCR. Asterisks indicate significant difference ($n = 3$ independent batches; $^{*}P < 0.05$; $^{**}P < 0.01$; $^{***}P < 0.005$; ns, not significant; ANOVA with Bonferroni post hoc test). (*C*) Representative images showing lentivirus-mediated EGFP expression (green) and DAPI (blue) staining in MEF, 4D, 3M, and 25M TTF. (*D*) Average plating efficiency (DAPI staining/field of view, normalized to MEF condition; *i*) and infection efficieny (percentage of EGFP^{+}/DAPI-stained cells; *ii*) calculated for MEF, 4D, 3M, and 25M TTF (left to right). Bar graphs represent mean ± SEM, and statistical significance were calculated by using ANOVA with Bonferroni post hoc test ($n = 3$ batches, $^{*}P < 0.05$, $^{**}P < 0.01$; ns, not significant). (Scale bars, 20 μm.)

NEUROSCIENCE

cells was seen in both MEFs and adult fibroblasts. Thus, the age-specific phenotype of FoxO3 cannot simply be explained by loss or compensation of other FoxO family members. These results suggest that FoxO3 direct transcriptional function heavily depends on the age-related cellular context and is fundamentally different in cultured MEFs than adult TTFs under otherwise identical growth conditions. It was described that FoxO3 regulates neural stem cell homeostasis only in adult but not embryonic or neonatal animals, a similar, age-dependent function of FoxO3 (19).

Here, we demonstrate the proof of principle that cells from old animals can still be converted to neurons without decline in efficiency with increased adult age. Because the most common diseases of the brain affect adult and elderly patients, this result is of relevance for potential applications of this technology in both disease modeling and regenerative medicine.

Experimental Procedures

Animals. All experimental procedures were approved by Stanford's administrative panel on laboratory animal care and were in accordance with national guidelines. Animals used for this project include WT C57BL/6 mice (Charles River or NIA colony) (Figs. 1 *C* and *D*, 2, 3, and 4 *A* and *D*, and Figs. S1–S3), and FoxO3 WT/KO mice (from Ronald A. DePinho, Dana–Farber Cancer Center, Boston, MA) (Figs. 1*B* and 4 *B*, *C*, and *E–G* and Figs. S4 and S5). FoxO3 KO mice were genotyped by PCR as described previously (25) before the start of all experiments. In addition, loss of *FoxO3* expression in TTFs was verified by qRT-PCR (Fig. S4*B*). For Fig. 1*A*, homozygous male Tau-EGFP mice (Jackson Laboratory) were bred with WT C57BL/6 mice and heterozygous offspring were used for experiments.

Cell Culture. Embryonic day 13.5 MEFs and postnatal fibroblasts were derived as described (1). Adult and aging fibroblasts were derived from mouse tails (TTF) by cutting the tissue into small pieces, followed by trypsin digestion, brief air drying on culture plates to enhance attachment, adding MEF media [DMEM high glucose, 10% (vol/vol) calf serum, 2 mM L-glutamine,1 mM sodium pyruvate, 0.1 mM nonessential amino acids, 50 U Penicillin-Streptomycin (Life Technologies) and β-mercaptoethanol (Sigma)] and subsequent isolation of fibroblast outgrowths. Fibroblasts from all ages were further expanded for 1–3 passages before reprogramming experiments. Primary hippocampal cultures were prepared from CD1 mice (Charles River) postnatal day 0–1.

Generation of iN Cells. For reprogramming experiments, fibroblasts were plated on Poly-ornitine/Laminin or Matrigel (BD Biosciences) coated dishes. Lentiviruses encoding the cDNAs for Ascl1-T2A-Brn2, Myt1l, and FoxO3 (driven by doxycycline-inducible Tet-on promoter) together with rtTA (under Ubiquitin promoter) were used to coinfect fibroblasts in MEF media in the presence of polybrene (8 mg/mL; Sigma). For knockdown experiments, cells were coinfected with pSico vectors

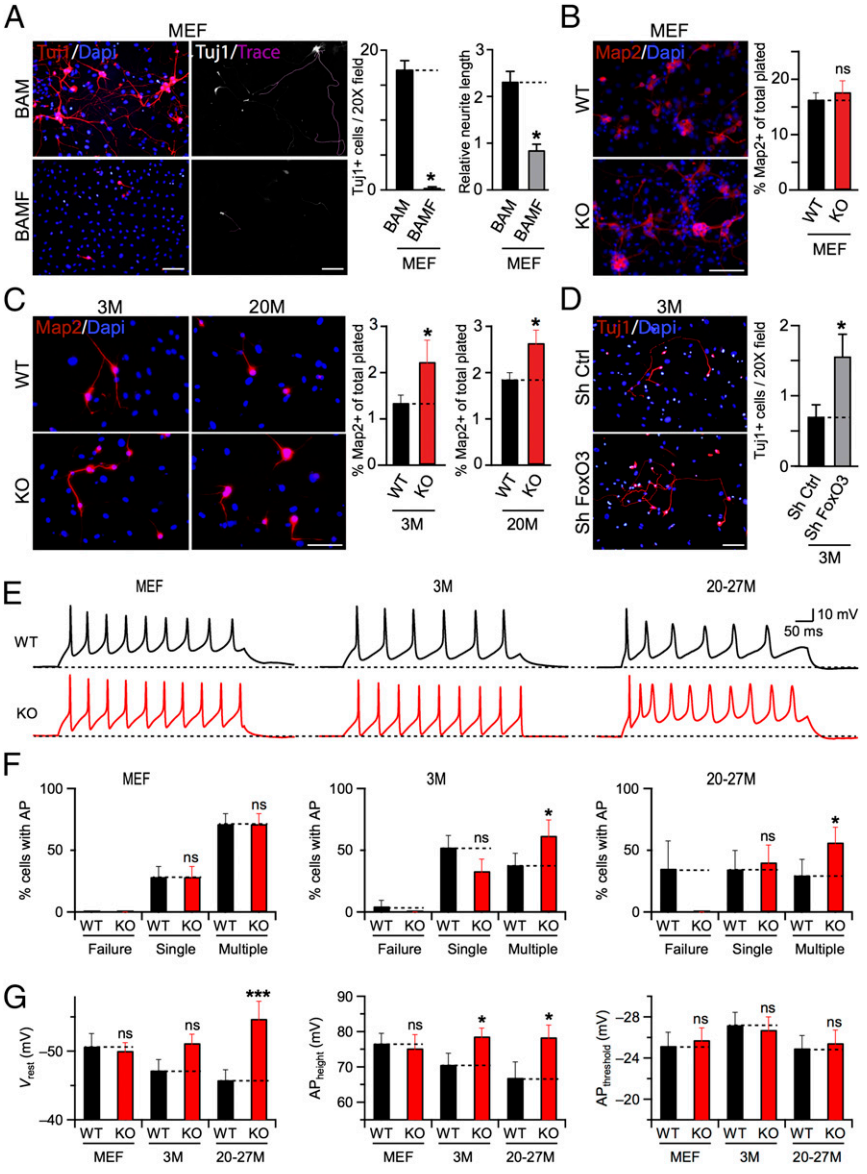

Fig. 4. Loss of FoxO3 improves reprogramming efficiency and functional maturation of iN cells derived from TTFs but not from MEFs. (*A*) Tuj1-immunoreactive, traced MEF iN cells derived in control condition (infected with BAM factors only, BAM; *Upper*) or in the presence of FoxO3 transcription factor (infected with BAM factors + FoxO3, BAMF; *Lower*). Bar graphs represent average values (means ± SEM, $n = 3$ batches, $^*P < 0.05$, ANOVA with Bonferroni post hoc test) of cell number and relative neurite length for each condition, as indicated. (*B*) Map2-immunoreactive MEF iN cells derived from WT (*Upper*) and FoxO3$^{-/-}$ (KO; *Lower*) littermate animals. Average percentages are means ± SEM, $n = 3$ experiments ($^*P < 0.05$, ANOVA with Bonferoni post hoc test). (*C*) Same as *B*, except for TTF iN cells derived from 3M (*Left*) and 20M (*Right*) old WT (*Upper*) or FoxO3 KO (*Lower*) animals. (*D*) Representative images (*Left*) of Tuj1$^+$ iN cells derived from 3M TTF, in the presence of shRNA hairpins for scrambled control (Sh Ctrl; *Upper*) or FoxO3 (Sh FoxO3; *Lower*). Average numbers of Tuj1$^+$ cells are plotted as means ± SEM (*Right*) for each condition, $n = 3$ technical replicates ($^*P < 0.05$, ANOVA with Bonferroni post hoc test). (*E*) Example traces of APs recorded from iN cells derived from MEF (*Left*), 3M (*Center*), and 20–27 M (*Right*) TTF of WT (*Upper*, black) or KO (*Lower*, red) mice. (*F*) Percentages (means ± SEM) of iN cells with no (Failure), single, or multiple APs recorded from MEF (*Left*), 3M (*Center*), and 20–27 M TTFs (*Right*). Asterisks indicate significant difference ($n = 3$ independent batches, $^*P < 0.05$, Student's *t* test) for pairwise comparison (dotted lines). ns, not significant. (*G*) Average values of the V_{rest}, AP height, and AP threshold of iN cells derived from MEF, 3M, and 20–27M TTFs ($n = 21$, 21, and 43, respectively, for each genotype). Asterisks, significant difference ($^*P < 0.05$, $^{***}P < 0.005$), ns, not significant, Student's *t* test. (Scale bars: 50 μm.)

carrying the shRNA of a scrambled control (ATCTCGCTTGGGCGAGAGT) or a FoxO3 (AAGCAGGCCTCATCTCAAA) sequence. The day after infection, MEF media was replaced with N3B27 media (DMEM/F12, N2, B27, 5 mg/mL insulin, doxycycline) with doxycycline (2 mg/mL; Sigma). The iN cell cultures were subsequently maintained with half media exchanges every 3 d. For cocultures with primary neurons, iN cells where enriched by infecting fibroblast with Ascl1-T2A-Brn2-ires-puro^r, Myt1l, rtTA, and eGFP. After 24 h of induction, cells were selected for 48 h, and after an additional 4 d, iN cells were dissociated and replated on 2- to 3-d in vitro mouse hippocampal cultures.

Electrophysiology. Electrophysiology experiments (current-clamp for AP generation, and voltage-clamp for synaptic recording) on TTF iN cells were performed essentially as described (9). In brief, EGFP$^+$ iN cells, only with elaborate neuronal morphology, were patched in whole-cell configuration by using internal solution containing: (for voltage-clamp) 135 mM $CsCl_2$, 10 mM Hepes, 1 mM EGTA, 1 mM Na-GTP, and 1 mM QX-314 (pH 7.4, 310 mOsm); or (for current-clamp) 130 mM $KMeSO_3$, 10 mM NaCl, 10 mM Hepes, 2 mM $MgCl_2$, 0.5 mM EGTA, 0.16 mM $CaCl_2$, 4 mM Na_2ATP, 0.4 mM NaGTP, and 14 mM Tris-creatine phosphate (pH 7.3, 310 mOsm). Extracellular solution contained 140 mM NaCl, 5 mM KCl, 2 mM $CaCl_2$, 1 mM $MgCl_2$, 10 mM glucose, and 10 mM Hepes-NaOH pH 7.4. Current-clamp recordings for AP generation were performed at approximately −60 mV, with a small holding current to adjust membrane potential accordingly. Voltage-clamp recordings for synaptic responses were at a holding potential of −70 mV. AMPAR-mediated synaptic responses were recorded in presence of picrotoxin ($GABA_AR$ blocker, 50 μM; Tocris). AMPAR-evoked EPSCs were isolated by using an extracellular stimulation electrode as described previously (26).

Immunocytochemistry. Cells were fixed with 4% paraformaldehyde, washed with PBS, incubated in T-PBS (PBS + 0.025% Triton X-100 + 5% serum) for 1 h at room temperature, then with desired primary antibodies at 4 °C overnight. Following washes, secondary antibodies were applied in T-PBS for 2 h at room temperature and finally washed with PBS. Primary antibodies used were as follows: mouse-anti-MAP2 (1:500, Sigma), rabbit anti-bIII Tubulin (Tuj1, 1:1000; Covance). Secondary antibodies used were donkey anti-mouse Alexa Fluor 555 and donkey-anti-rabbit Alexa Fluor 488 (1:1000; Life Technologies). For EdU staining, cells were pulsed with 10 mM EdU for 4 h and visualized by using ClickIT EdU kit (Life Technologies) according to manufacturer guidelines. SA-β-Gal staining was performed by using the senescencent cell staining kit (Sigma) according to the manufacturer's guidelines. Nuclear counterstaining was performed with DAPI.

Cell Quantification and Neurite Length Measurements. The conversion efficiencies for TTF iN cells from different age groups and genotypes were determined by counting total number of Tuj1$^+$ and Map2$^+$ cells with clear neuronal morphology in 20 random 20× field of views and presented as percentages of total plated cells. EdU$^+$ and SA-β-Gal$^+$ cells were counted in 10 random 40× field of views and indicated as average percentage of total DAPI-stained nucleus. Neurite length measurements were performed on randomly selected 10× Tuj1$^+$ iN cell images by using the ImageJ software (NIH) with NeuronJ plug-in.

qRT-PCR. Total RNA was isolated by using RNAeasy (Qiagen) with DNase treatment, reverse transcribed by using SuperScript II (Life Technologies) with oligo dT and qPCR performed with the 7900HT Real Time PCR system using SYBR green master mix (Applied Biosystems) and the following primers (for Fig. 3B and Fig. S5*B*):

GAPDH-Fwd: 5′tgtgtccgtcgttggatctga3′,

GAPDH-Rev: 5′ttgctgttgaagtcgcaggag3′,

p16-Fwd: 5′CGAACTCTTTCGGTCGTACCC3′,

p16-Rev: 5′CGAATCTGCACCGTAGTTGAGC3′,

p19-Fwd: 5′GTTCTTGGTCACTGTGAGGATTCAG3′, and

p19-Rev: 5′CCATCATCATCACCTGGTCCAG3′.

Additional primer information for FoxO3 KO validation and testing its subsequent effect on other FoxO family members is provided in Fig. S4.

Statistical Analyses. All average bar-graph data are presented as means ± SEM. Statistical comparisons were made by using ANOVA with Bonferroni post hoc test (*$P < 0.05$, **$P < 0.01$, and ***$P < 0.005$) or two-tailed, unpaired Student *t* test (except for Fig. 4*F*, where a paired *t* test was performed), as individually mentioned in the figure legends.

ACKNOWLEDGMENTS. We thank Ronald DePinho for the FoxO3 knockout mice, the members of the A.B. laboratory for sharing aged mice, and members of the M.W. laboratory for reagents and helpful discussions. This study was supported by NIH Grants AG010770-18A1 (to M.W., T.C.S., and S.B.P.) and R01MH092931 (to M.W. and T.C.S.); Swedish Research Council and Swedish Society for Medical Research Postdoctoral fellowships (to H.A.); and Stanford Institute for Chemical Biology Postdoctoral Grant ChEM-H112878 (to S.C.). T.C.S. is a Howard Hughes Medical Institute Investigator, and M.W. is a New York Stem Cell Foundation-Robertson Investigator and a Tashia and John Morgridge Faculty Scholar, Child Health Research Institute at Stanford.

1. Vierbuchen T, et al. (2010) Direct conversion of fibroblasts to functional neurons by defined factors. *Nature* 463(7284):1035–1041.
2. Marro S, et al. (2011) Direct lineage conversion of terminally differentiated hepatocytes to functional neurons. *Cell Stem Cell* 9(4):374–382.
3. Cheng Z, et al. (2011) Establishment of induced pluripotent stem cells from aged mice using bone marrow-derived myeloid cells. *J Mol Cell Biol* 3(2):91–98.
4. Ambasudhan R, et al. (2011) Direct reprogramming of adult human fibroblasts to functional neurons under defined conditions. *Cell Stem Cell* 9(2):113–118.
5. Yoo AS, et al. (2011) MicroRNA-mediated conversion of human fibroblasts to neurons. *Nature* 476(7359):228–231.
6. Victor MB, et al. (2014) Generation of human striatal neurons by microRNA-dependent direct conversion of fibroblasts. *Neuron* 84(2):311–323.
7. Caiazzo M, et al. (2011) Direct generation of functional dopaminergic neurons from mouse and human fibroblasts. *Nature* 476(7359):224–227.
8. Pfisterer U, et al. (2011) Direct conversion of human fibroblasts to dopaminergic neurons. *Proc Natl Acad Sci USA* 108(25):10343–10348.
9. Chanda S, Marro S, Wernig M, Südhof TC (2013) Neurons generated by direct conversion of fibroblasts reproduce synaptic phenotype caused by autism-associated neuroligin-3 mutation. *Proc Natl Acad Sci USA* 110(41):16622–16627.
10. Li H, et al. (2009) The Ink4/Arf locus is a barrier for iPS cell reprogramming. *Nature* 460(7259):1136–1139.
11. Kim K, et al. (2010) Epigenetic memory in induced pluripotent stem cells. *Nature* 467(7313):285–290.
12. Wang B, et al. (2011) Reprogramming efficiency and quality of induced Pluripotent Stem Cells (iPSCs) generated from muscle-derived fibroblasts of mdx mice at different ages. *PLoS Curr* 3:RRN1274.
13. Mertens J, et al. (2015) Directly reprogrammed human neurons retain aging-associated transcriptomic signatures and reveal age-related nucleocytoplasmic defects. *Cell Stem Cell* 17(6):705–718.
14. Chanda S, et al. (2014) Generation of induced neuronal cells by the single reprogramming factor ASCL1. *Stem Cell Rep* 3(2):282–296.
15. Wapinski OL, et al. (2013) Hierarchical mechanisms for direct reprogramming of fibroblasts to neurons. *Cell* 155(3):621–635.
16. Webb AE, et al. (2013) FOXO3 shares common targets with ASCL1 genome-wide and inhibits ASCL1-dependent neurogenesis. *Cell Reports* 4(3):477–491.
17. Paik JH, et al. (2009) FoxOs cooperatively regulate diverse pathways governing neural stem cell homeostasis. *Cell Stem Cell* 5(5):540–553.
18. Kenyon CJ (2010) The genetics of ageing. *Nature* 464(7288):504–512.
19. Renault VM, et al. (2009) FoxO3 regulates neural stem cell homeostasis. *Cell Stem Cell* 5(5):527–539.
20. Tucker KL, Meyer M, Barde YA (2001) Neurotrophins are required for nerve growth during development. *Nat Neurosci* 4(1):29–37.
21. Ahlenius H, Visan V, Kokaia M, Lindvall O, Kokaia Z (2009) Neural stem and progenitor cells retain their potential for proliferation and differentiation into functional neurons despite lower number in aged brain. *J Neurosci* 29(14):4408–4419.
22. Banito A, et al. (2009) Senescence impairs successful reprogramming to pluripotent stem cells. *Genes Dev* 23(18):2134–2139.
23. Ruiz S, et al. (2011) A high proliferation rate is required for cell reprogramming and maintenance of human embryonic stem cell identity. *Curr Biol* 21(1):45–52.
24. Furuyama T, et al. (2002) Effects of aging and caloric restriction on the gene expression of Foxo1, 3, and 4 (FKHR, FKHRL1, and AFX) in the rat skeletal muscles. *Microsc Res Tech* 59(4):331–334.
25. Castrillon DH, Miao L, Kollipara R, Horner JW, DePinho RA (2003) Suppression of ovarian follicle activation in mice by the transcription factor Foxo3a. *Science* 301(5630):215–218.
26. Maximov A, Pang ZP, Tervo DG, Südhof TC (2007) Monitoring synaptic transmission in primary neuronal cultures using local extracellular stimulation. *J Neurosci Methods* 161(1):75–87.